

# Facile Aqueous Synthesis of CeO<sub>2</sub> Octahedrons for Memristor Application

Haiwei Du<sup>1</sup>, Bo Qu<sup>1</sup>, Tao Wan<sup>1</sup>, Jianchao Chen<sup>2</sup>, Dewei Chu<sup>1</sup>

<sup>1</sup> School of Materials Science and Engineering, University of New South Wales

UNSW, High Street, Kensington, NSW 2052, Australia

Phone: +61-402092934 E-mail: [haiwei.du@student.unsw.edu.au](mailto:haiwei.du@student.unsw.edu.au) (H. Du), [d.chu@unsw.edu.au](mailto:d.chu@unsw.edu.au) (D. Chu)

<sup>2</sup> Institute for Materials Research, Tohoku University, 2-1-1 Katahira, Aoba-ku, Sendai 980-8577, Japan

## Abstract

Nanostructured ceria-based materials exhibit important commercial utility in various fields. The desired morphology with specific crystal facets and intrinsic defect (oxygen vacancies) offer the opportunity for designing novel electronic devices. In this study, CeO<sub>2</sub> nano-octahedrons were synthesized via a facile hydrothermal method without using mineralizers. The TEM results showed that CeO<sub>2</sub> crystals are enclosed by {111} facet with the lowest surface energy. Furthermore, CeO<sub>2</sub> nano-octahedron-based resistive switching memory devices were fabricated by self-assembly route and the devices showed good bipolar resistance switching characteristics.

## 1. Introduction

Resistive random access memory (RRAM) with simple capacitor-like structure, nonvolatility, low power consumption, and high write/erase speed, has been considered as one of the next-generation nonvolatile memory technique [1]. However, conventional fabricating methods are faced with several urgent problems such as large-scale production, relatively high cost and difficulty in further miniaturization. Fortunately, bottom-up approaches, especially for functional oxide materials, provide an alternative strategy for RRAM device fabrication [2]. Among these oxides, CeO<sub>2</sub> (ceria) shows promising potential in RRAM applications since the oxygen vacancies resulting from the intrinsic charge transfer between two oxidation states (Ce<sup>3+</sup>/Ce<sup>4+</sup>) [3] can migrate under electric field because of their high activity and mobility. The previous work of our group [4] has reported that the excellent RRAM properties can be achieved in CeO<sub>2</sub> nanocubes, in which the oxygen vacancies act as the conductive filament for resistive switching (RS). In the present work, a memory device based on CeO<sub>2</sub> octahedrons is fabricated, and bipolar RS behavior is observed.

## 3. Results and Discussions

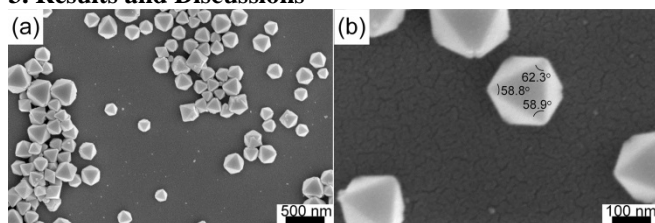


Fig. 1 Scanning electron microscopy (SEM) images (a, b) of CeO<sub>2</sub> octahedrons synthesized at 200 °C for 24 h.

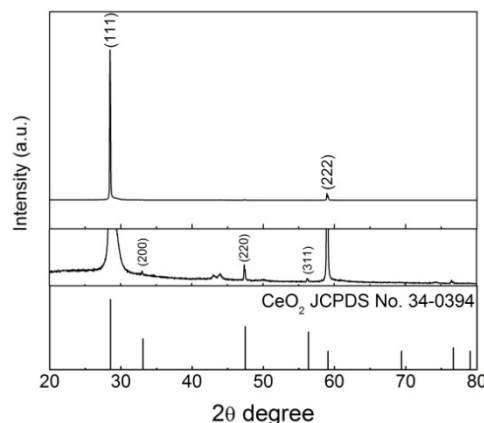


Fig. 2 XRD pattern of CeO<sub>2</sub> octahedrons.

Fig. 1 shows the SEM images of CeO<sub>2</sub> crystals with high symmetry octahedron morphology and the edge length from 100 to 300 nm. The measured dihedral angles of a typical octahedron in Fig. 1b are about 58.8°, 62.3° and 58.9°, respectively, which are close to the theoretical value of 60°. Meanwhile, the surface of octahedrons is enclosed by {111} facet and this is also confirmed by X-ray diffraction (XRD) characterization. As shown in Fig. 2, two obvious peaks corresponding to (111) and (222) which are in agreement with the standard pattern of CeO<sub>2</sub> (JCPDS No. 34-0394) show high intensity while (200), (220) and (311) can be detected with very low intensity. The lattice parameter from XRD result is calculated to be 5.4222 Å.

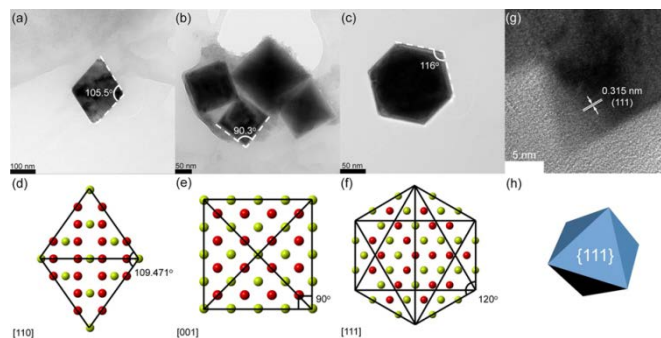


Fig. 3 TEM images of CeO<sub>2</sub> octahedrons recorded from the [110] (a), [001] (b) and [111] (c) zone axis. The atomic structures of the CeO<sub>2</sub> viewed along [110] (d), [001] (e) and [111] (f) directions. HRTEM of CeO<sub>2</sub> octahedron (g) and schematic of octahedron (h).

More-detailed structural information on the octahedral  $\text{CeO}_2$  particles is provided by transmission electron microscopy (TEM), as shown in Fig. 3(a-d). The TEM images of octahedron nanoparticles viewed along [110], [001] and [111] zone axis show parallelogram, square and hexagon morphologies, and the included angles are  $105.5^\circ$ ,  $90.3^\circ$  and  $116^\circ$  respectively, matching well with the theoretical value of  $109.471^\circ$ ,  $90^\circ$  and  $120^\circ$ . Furthermore, the lattice spacing parallel to facets measured from HRTEM image is 0.315 nm, corresponding to the (111) plane of  $\text{CeO}_2$ . Therefore, the above characterizations prove that the as-synthesized  $\text{CeO}_2$  particles are exposed with {111} facets.

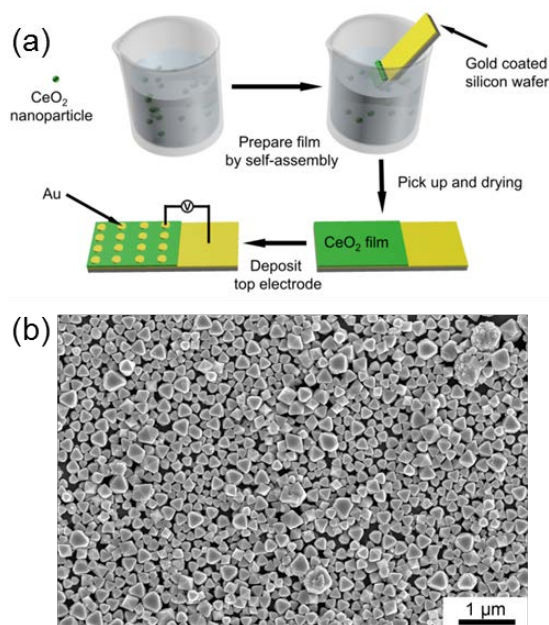


Fig. 4 Schematic of self-assembly process for preparing  $\text{CeO}_2$  RRAM device (a) and SEM image of  $\text{CeO}_2$  film (b).

The RRAM device was fabricated by self-assembly route. As shown in Fig. 4a, the  $\text{CeO}_2$  particles were firstly dispersed in ethanol and then a gold-coated silicon substrate was immersed into the particle solution under ambient condition until 2/3 region with the electrodes was soaked. After the evaporation, the substrate was picked up and finally dried at  $50^\circ\text{C}$  for 2 h. Finally, patterned Au electrode with size of about  $250\ \mu\text{m}$  in diameter was sputtered through a shadow mask onto the devices.

The current - voltage ( $I - V$ ) characteristics of the  $\text{CeO}_2$  memory cell were carried out by dc voltage sweep in the sequence of  $0 \rightarrow +5 \rightarrow 0 \rightarrow -5 \rightarrow 0\ \text{V}$ , and the results are illustrated in semilogarithmic scales (Fig. 5a). The high resistance state (HRS, OFF) is converted to low resistance state (LRS, ON) at about 2.8 V, corresponding to “SET” process. This ON state is maintained and switched to HRS when applying negative bias, which is “RESET” process, indicating bipolar resistive switching nature of the device. It is seen that a two-step switching from LRS to HRS takes place at  $-3.7\ \text{V}$  and  $-4.9\ \text{V}$ . The resistances of each LRS and HRS during 500 cycles are measured at 0.5 V (Fig. 5b), and the on/off ratio is approximately 80. As no resistance fluctu-

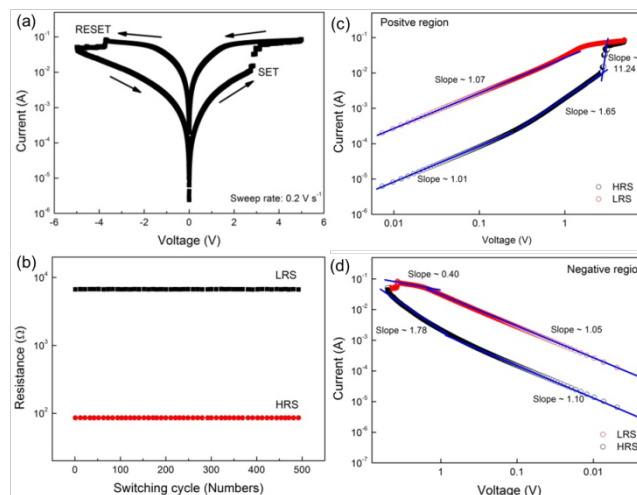


Fig. 5 Typical current-voltage ( $I - V$ ) characteristic of Si/Au/ $\text{CeO}_2$ /Au device in semi-logarithmic scale (a). Sweep rate:  $0.2\ \text{V s}^{-1}$ . Endurance characteristic of Si/Au/ $\text{CeO}_2$ /Au device (b). Readout at 0.5 V. Replots of  $\log I$  vs  $\log V$  in Fig. 5(a) under positive (c) and negative bias (d), fitted for conduction mechanism.

ations at ON and OFF states are observed during endurance test, our device shows reliable memory property.

To further understand the conducting behaviour in  $\text{CeO}_2$  device, nonlinear  $I - V$  characteristics are plotted in a log-log scale. The fitting results exhibit Ohmic conduction with slope  $\sim 1$  in LRS state, confirming the formation of conductive path during SET process. While for HRS state, the charge transport is similar to space charge limited conduction (SCLC), suggesting that high conductivity in ON state is attributed to filament effect rather than a homogeneously distributed one.

## 4. Conclusions

In summary,  $\text{CeO}_2$  octahedrons are synthesized by a facile aqueous method. The resistive switching device based on  $\text{CeO}_2$  octahedrons by self-assembly route exhibit bipolar switching behaviour and the device is promising for non-volatile memory since the solution processed approach enables large-area device production.

## Acknowledgements

This work is funded by the Australian Research Council Project (grant no. FT140100032). H. Du thanks China Scholarship Council (CSC) for financial support (no. 201406410060).

## References

- [1] F. Pan, S. Gao, C. Chen, C. Song and F. Zeng, Mater. Sci. Eng.: R: Rep. **83** (2014) 1.
- [2] J.-S. Lee, J. Mater. Chem. **21** (2011) 14097.
- [3] D. Mullins, S. Overbury and D. Huntley, Surf. Sci. **409** (1998) 307.
- [4] A. Younis, D. Chu, I. Mihail and S. Li, ACS Appl. Mater. Interfaces **5** (2013) 9429.